Altering kinetic mechanism and enzyme stability by mutagenesis of the dimer interface of glutathione reductase

Asam BASHIR, Richard N. PERHAM, Nigel S. SCRUTTON* and Alan BERRY†‡
Cambridge Centre for Molecular Recognition, Department of Biochemistry, University of Cambridge, Tennis Court Road, Cambridge CB2 1QW, U.K.

In wild-type glutathione reductase from *Escherichia coli* residues Val^{421} and Ala^{422} are located in an α-helix in a densely packed and hydrophobic region of the dimer interface, with their side chains packed against those of residues $Ala^{422'}$ and $Val^{421'}$ in the second subunit. A series of mutant glutathione reductases was constructed in which the identities of the residues at positions 421 and 422 were changed. Mutations were designed so as to present like charges (mutants $Val^{421} \rightarrow Glu$:$Ala^{422} \rightarrow Glu$ and $Val^{421} \rightarrow Lys$:$Ala^{422} \rightarrow Lys$) or opposite charges (mutant $Val^{421} \rightarrow Lys$:$Ala^{422} \rightarrow Glu$) across the dimer interface to assess the role of electrostatic interactions in dimer stability. A fourth mutant ($Val^{421} \rightarrow His$:$Ala^{422} \rightarrow His$) was also constructed to investigate the effects of introducing a potentially protonatable bulky side chain into a crowded region of the dimer interface. In all cases, an active dimeric enzyme was found to be assembled but each mutant protein was thermally destabilized. A detailed steady-state kinetic analysis indicated that each mutant enzyme no longer displayed the Ping Pong kinetic behaviour associated with the wild-type enzyme but exhibited what was best described as a random bireactant ternary complex mechanism. This leads, depending on the chosen substrate concentration, to apparent sigmoidal, hyperbolic or complex kinetic behaviour. These experiments, together with others reported previously, indicate that simple mutagenic changes in regions distant from the active site can lead to dramatic switches in steady-state kinetic mechanism.

INTRODUCTION

Escherichia coli glutathione reductase (EC 1.6.4.2) is a homodimeric flavoenzyme containing 450 amino acid residues [1] with 1 FAD per subunit, and it catalyses the reduction of oxidized glutathione (GSSG) according to the equation:

$$GSSG + NADPH + H^+ = 2GSH + NADP^+$$

Glutathione reductase is important in maintaining the redox balance within the cell [2], and reduced glutathione (GSH) is involved in various important cellular functions [3]. The *E. coli* enzyme has been the subject of many site-directed mutagenesis experiments including the insertion of an intersubunit disulphide bridge [4], the identification of catalytically important residues and a switch of kinetic mechanism from Ping Pong to ordered sequential [5–8], the switch of coenzyme specificity from NADPH to NADH [9], and a change of substrate specificity from glutathione to trypanothione [10]. The enzyme has also been used to demonstrate the possibility of excising individual protein domains by rational redesign of newly exposed hydrophobic surfaces [11].

The crystal structures of the wild-type enzyme [12] and various mutant forms [13,14] have been solved at high resolution. The protein is typical of the family of flavoprotein disulphide oxidoreductases in that each subunit contains four well-delineated domains: from the N-terminus, an FAD-binding domain, an NADP-binding domain, a central domain and an interface domain. The two active sites are at the dimer interface, related by a two-fold axis of symmetry, with the substrate glutathione bound by residues contributed by both subunits. Thus only the dimeric form of the enzyme can be catalytically active. The dimer interface comprises two regions. The upper interface, contributed largely by the interface domain, makes a large contact with its counterpart in the opposing subunit, whereas the smaller lower interface is formed by a contact between two α-helical extensions protruding from the FAD-binding domain. The upper interface region forms one of the most rigid parts of the protein and, although more hydrophobic than the lower region, forms about 75% of the intersubunit hydrogen-bonds. The tightest packing within the upper interface region is centred on an α-helix consisting of residues 412 to 424, which is juxtaposed to its counterpart in the opposing subunit. Water plays an important role in the structure of the dimer interface with a water-filled cavity between the upper and lower interface regions [12]. The importance of the upper interface in dimer assembly is borne out by the high degree of sequence conservation in glutathione reductase from different species (93% sequence identity between *E. coli* and human glutathione reductases), whereas the lower interface is relatively poorly conserved (32% identity between the *E. coli* and human enzymes).

In previous work, we demonstrated that mutation of a single amino acid residue in the upper dimer interface of *E. coli* glutathione reductase ($Gly^{418} \rightarrow Trp$) led to the assembly of a less stable enzyme dimer [7]. The kinetic properties of the $Gly^{418} \rightarrow Trp$ mutant were also markedly altered: the hyperbolic kinetic behaviour of the wild-type enzyme was replaced by highly sigmoidal behaviour (Hill coefficient 1.8) with respect to the second substrate, glutathione [7]. The structural basis for this change in kinetic behaviour is not yet understood but it probably reflects side-chain and/or backbone rearrangements at the dimer interface that are felt in distal parts of the enzyme. In this paper we describe the effects of further mutations in the two α-helices located in the upper interface region that pack against each other in the dimer. Specifically, replacements of Val^{421} and Ala^{422} were introduced to juxtapose like charges across the interface and

* Present address: Department of Biochemistry, University of Leicester, Adrian Building, University Road, Leicester LE1 7RH, U.K.
† Present address: Department of Biochemistry and Molecular Biology, University of Leeds, Leeds LS2 9JT, U.K.
‡ To whom correspondence should be addressed.

thereby to interfere with dimer assembly. Active dimeric enzymes are still formed and, in the presence of a relatively low concentration of NADPH, they display highly sigmoidal kinetic behaviour with respect to glutathione concentration. With higher concentrations of NADPH, however, the kinetic behaviour is hyperbolic. We show that a bireactant-random ternary complex kinetic scheme is consistent with the observed behaviour and that this additional complexity in kinetic behaviour is achieved at the expense of lower thermal stabilities for the mutant enzymes.

MATERIALS AND METHODS

Materials

Bacteriological media were from Difco Laboratories and all media were prepared as described in Sambrook et al. [15]. Ethidium bromide was purchased from Bachem. Ultrapure agarose and CsCl were from Bethesda Research Laboratories. Glutathione and NADPH were from Sigma. Ampicillin was from Beecham Research Laboratories. All other chemicals were of analytical grade wherever possible. Glass-distilled water was used throughout.

Restriction enzymes *Eco*RI, *Bss*HII and *Hin*dIII were purchased from Pharmacia LKB Biotechnology Inc. Calf intestinal alkaline phosphatase was obtained from Boehringer Mannheim. T4 DNA ligase and T4 polynucleotide kinase were from Amersham International. *E. coli* strain TG1 [r_k^-, m_k^-, *rec* A1, *sup* E, *end* A1, *hsd* R17, *gyr* A96, *rel* A1, *thi*, Δ(lac-pro AB)/F′ *tra* D36, *pro* A^+B^+, *lac* i^q, *lac* Z ΔM15] was from Amersham International. Strains NS3 [Δ(*his-gnd*), Δ*gor*, Δ*lac*, *ara* D, *pro*$^-$/F′ *tra* D36, *pro* A^+B^+, *lac* I^q, *lac* Z ΔM15], which lacks a chromosomal copy of the *gor* gene, and the proteinase-deficient strain NA33 [*lac*(amb), *tyr*(amb), *pho*(amb), *sup* C(ts), Str^R, *htp* R$^-$, lCI_{857}, Δ*int*(C3-H1), ΔBam, Tet^R(tn10), *gal* E, *bio*$^-$, *uvr* B$^-$/F′ *tra* D36, *pro* A^+B^+, *lac* I^q, *lac* Z ΔM15] have been described elsewhere [5,16].

Mutagenesis, plasmid construction and DNA sequencing

Bacteria were cultured in 2 × YT medium [15] supplemented, where appropriate, with ampicillin and streptomycin. Bacteriophage replicative-form DNA and plasmid DNA were prepared by CsCl density centrifugation [15]. For the purposes of screening, plasmids were prepared on a miniscale with the Wizard DNA purification kit (Promega, U.K.). Restriction endonuclease digestion and ligation of DNA were carried out as recommended by the enzyme suppliers.

For the isolation of mutants $Val^{421} \rightarrow Lys:Ala^{422} \rightarrow Lys$ and $Val^{421} \rightarrow Glu:Ala^{422} \rightarrow Glu$, site-directed mutagenesis was performed on a derivative of M13 containing the non-coding strand of the *gor* gene exactly as described previously [5] with the mutagenic oligonucleotides 5′-AGG GCT TCG CGA AAA AAC TGA AGA TGG G-3′ ($Val^{421} \rightarrow Lys:Ala^{422} \rightarrow Lys$) and 5′-AGG GCT TCG CGG AGG AGC TGA AGA TGG G-3′ ($Val^{421} \rightarrow Glu:Ala^{422} \rightarrow Glu$). All mutant genes were fully resequenced using a T7 DNA sequencing system (Pharmacia) or an automated fluorescent sequencing facility (operated by Mr. J. Lester) to ensure that spurious mutations had not arisen during the mutagenesis reactions. Mutant genes were subcloned as *Eco*RI/*Hin*dIII fragments into the expression construct pKGR4, as described by Scrutton et al. [17]. The construction of mutants $Val^{421} \rightarrow His:Ala^{422} \rightarrow His$ and $Val^{421} \rightarrow Lys:Ala^{422} \rightarrow Glu$ was achieved with PCR. The template used was double-stranded plasmid pKGR4 [5]. PCR was performed under mineral oil in a reaction buffer (100 μl) containing 100 ng of double-stranded plasmid DNA, 200 μM dNTPs, 2 mM $MgCl_2$, 100 pmol of each sense and antisense primer, and 2.5 units of *Pfu* DNA polymerase (Stratagene) on a programmable PHC-3 thermal cycler (Techne Corp.). Sense primers containing the desired mutations were 5′-

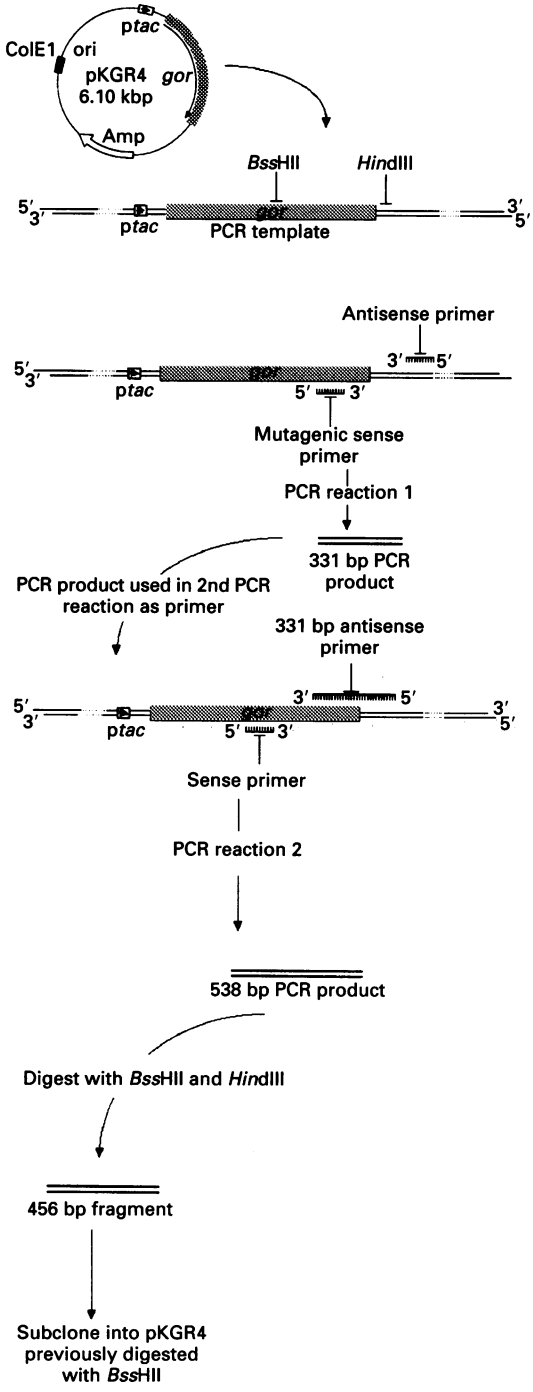

Figure 1 Creation of genes encoding the $Val^{421} \rightarrow Lys:Ala^{422} \rightarrow Glu$ and the $Val^{421} \rightarrow His:Ala^{422} \rightarrow His$ mutants of *E. coli* glutathione reductase

Sequences of the primers used in the PCR and other experimental details are described in detail in the text. Genes are shown by differential shading, and the orientations of genes and promoter are indicated with arrows. Amp, ampicillin resistance gene; Col E1 ori, origin of plasmid replication; p*tac*, *tac* promoter; *gor*, glutathione reductase gene. Positions of the *Bss*HII and *Hin*dIII sites are shown relative to the *gor* gene.

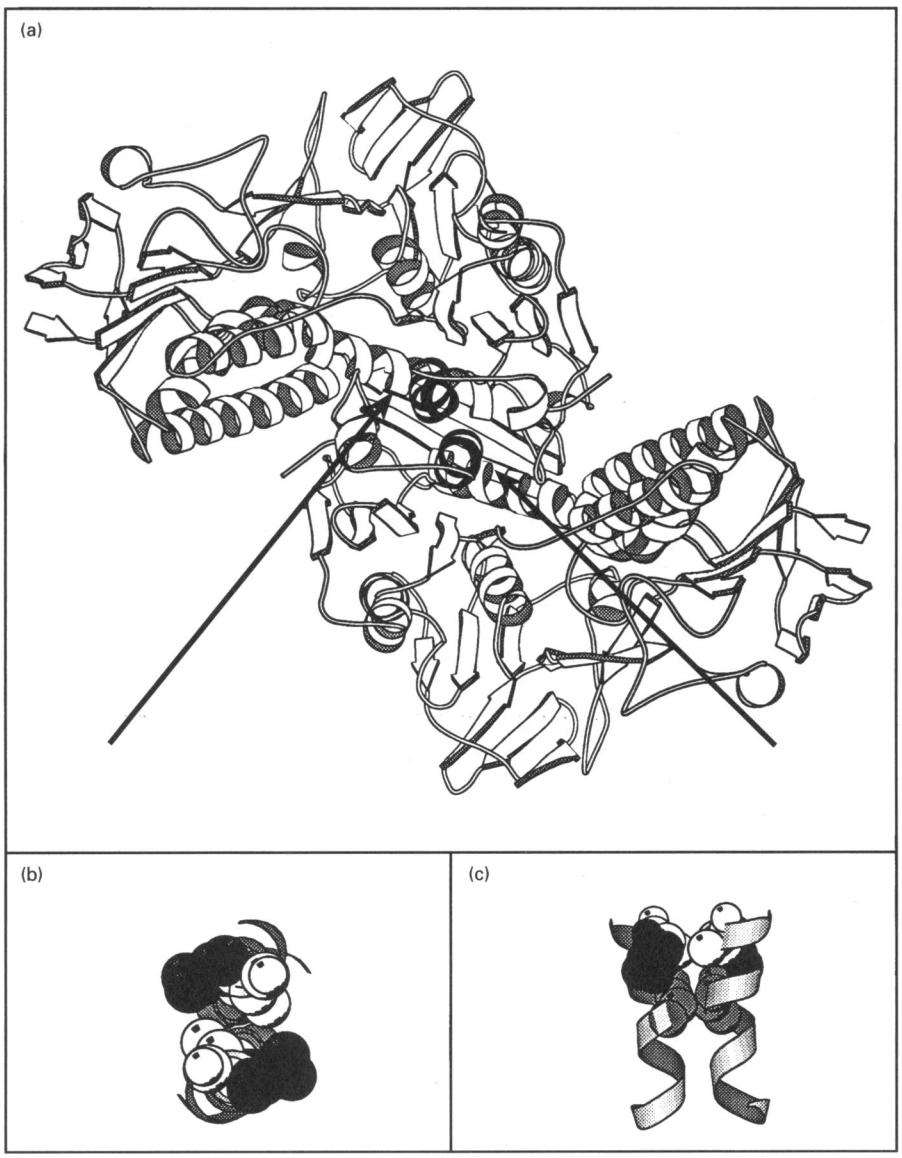

Figure 2 Representation of the dimer interface of *E. coli* glutathione reductase

The positions of residues G^{418}, Val^{421} and Ala^{422} are indicated. The structure was generated by the program MOLSCRIPT [24]. Coordinates were taken from the entry PDB1GET in the Brookhaven Protein Databank. (**a**) The dimeric structure of *E. coli* glutathione reductase. (**b**,**c**) Orthogonal views of helix 412–424, which lies at the centre of the dimer interface, showing the tight packing of residues in this area. Individual residues are shown as a CPK representation with sphere size equal to the van der Waals radius. Gly^{418} and $Gly^{418'}$ are shaded grey, Val^{421} and $Val^{421'}$ are shaded black and Ala^{422} and $Ala^{422'}$ are shown in white.

GGC TTC GCG CAC CAC CTG AAG ATG GG-3′ (Val^{421} → His:Ala^{422} → His) and 5′-GGC TTC GCG AAA GAG CTG AAG ATG GG-3′ (Val^{421} → Lys:Ala^{422} → Glu). These were used in combination with the antisense primer 5′-CCA TCC GCC GAT TGG TAC TGT TG-3′ which annealed to a region of the template on the 3′-side of a unique *Hin*dIII site downstream of the *gor* gene (Figure 1). The cycling parameters for the first reaction were as follows: 4 min at 95 °C (one cycle); 1 min at 94 °C, 2 min at 50 °C, and 3 min at 72 °C (25 cycles); and 10 min at 72 °C (one cycle).

The 331 bp double-stranded PCR product was isolated from a 3% (w/v) low-melting-temperature agarose gel using the Promega Wizard PCR purification system. This PCR product was used as a primer in a second PCR reaction together with the primer 5′-TCA GGC TGA AAA TCT TCT CTC ATC CG-3′, which annealed to a region of the template 5′ to a unique *Bss*HII site in the *gor* gene (Figure 1). The cycling parameters for the second PCR reaction were as follows: 4 min at 95 °C (one cycle); 1 min at 94 °C, 2 min at 62 °C, and 1.5 min at 72 °C (25 cycles); and 10 min at 72 °C (one cycle). The resulting 538 bp product was digested with *Bss*HII and *Hin*dIII and isolated after electrophoresis in a 4.5% polyacrylamide gel using the crush-and-soak method [15]. This fragment was subsequently subcloned into the glutathione reductase expression vector pKGR4 previously digested with *Bss*HII and *Hin*dIII (Figure 1). Each construct was resequenced to check for spurious mutations arising during the mutagenesis procedure. The construction of the Gly^{418} → Trp mutant of glutathione reductase has been described elsewhere [7].

Purification and characterization of wild-type and mutant enzymes

Recombinant enzymes were expressed from the appropriate plasmid-based system in *E. coli* strain NS3 and purified to homogeneity by a modification of the procedure previously described [5]. After ion-exchange chromatography on DE-52, samples were dialysed against 20 mM Mops buffer, pH 7.6, containing 1 mM EDTA (buffer A). Enzymes were further purified by affinity chromatography using a column of 2′,5′-ADP Sepharose 6B equilibrated with buffer A. The column was developed with a linear gradient (0 to 1.5 M) of KCl contained in buffer A and enzyme was eluted at a KCl concentration of 0.9 M. FAD (1 μM) was included in all buffers for the purification of mutant enzymes. Mutant $Val^{421} \rightarrow His:Ala^{422} \rightarrow His$ was found to be susceptible to proteolytic degradation when purified from strain NS3. This enzyme was therefore purified from a proteinase-deficient strain of *E. coli* (strain NA33; [16]) using the procedure described above.

Protein samples were submitted to SDS/10% (w/v) PAGE [18] and non-denaturing 12.5% (w/v) PAGE [19,20], and protein was revealed by staining with Coomassie Brilliant Blue R250. After exhaustive dialysis of purified enzymes against 100 mM potassium phosphate buffer, pH 7.6, the concentration of glutathione reductase was measured spectrophotometrically with an absorption coefficient of 11 300/M per cm at 462 nm for enzyme-bound FAD [5].

Steady-state kinetic measurements of wild-type and mutant glutathione reductases were conducted in 100 mM potassium phosphate buffer, pH 7.6, at 30 °C on a Kontron 930 Uvikon spectrophotometer [17]. Data were fitted to the appropriate rate equations with the computer program Kaleidograph (Abelbeck Software, CA). Assays of enzymes for thermal stability were performed as described by Scrutton et al. [4].

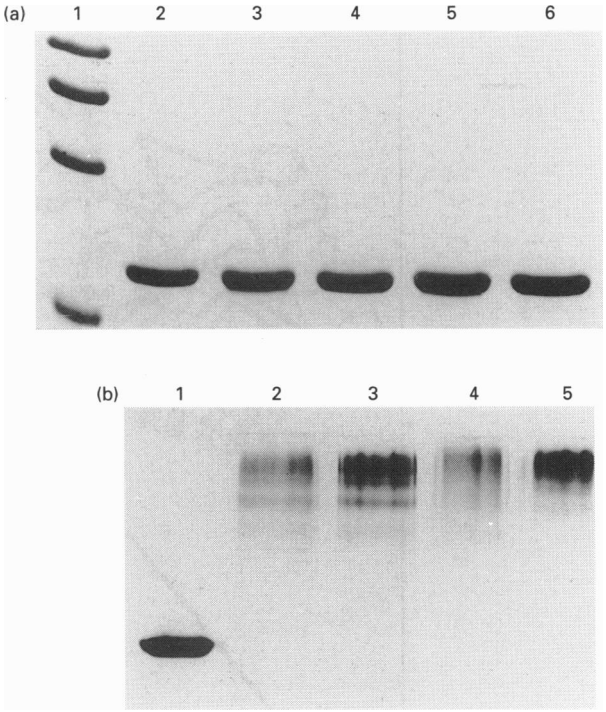

Figure 3 PAGE of purified wild-type and mutant glutathione reductases

(**a**) SDS/10% (w/v) PAGE analysis of purified enzymes. Lane 1, markers (116, 97.4, 66 and 45 kDa); lane 2, wild-type glutathione reductase; lane 3, $Val^{421} \rightarrow Lys:Ala^{422} \rightarrow Lys$ mutant; lane 4, $Val^{421} \rightarrow Glu:Ala^{422} \rightarrow Glu$ mutant; lane 5, $Val^{421} \rightarrow His:Ala^{422} \rightarrow His$ mutant; lane 6, $Val^{421} \rightarrow Lys:Ala^{422} \rightarrow Glu$ mutant. (**b**) 12.5% (w/v) non-denaturing PAGE analysis of purified enzymes. Lane 1, wild-type glutathione reductase; lane 2, $Val^{421} \rightarrow Lys:Ala^{422} \rightarrow Lys$ mutant; lane 3, $Val^{421} \rightarrow Glu:Ala^{422} \rightarrow Glu$ mutant; lane 4, $Val^{421} \rightarrow His:Ala^{422} \rightarrow His$ mutant; lane 5, $Val^{421} \rightarrow Lys:Ala^{422} \rightarrow Glu$ mutant.

RESULTS AND DISCUSSION

The dimer interface and residues Val^{421} and Ala^{422}

Previous experiments [7] with *E. coli* glutathione reductase have shown that juxtaposing two large residues in a tightly packed region of the interface (mutant $Gly^{418} \rightarrow Trp$) was insufficient to prevent the formation of active dimeric enzyme. However, a decreased thermal stability of the protein was observed. The upper interface region, which contains the $Gly^{418} \rightarrow Trp$ mutation, is evidently malleable enough to accept additional large hydrophobic side chains in what is itself a hydrophobic region of the protein. The introduction of electrostatic interactions in this same region of the interface might have different effects, and therefore a series of appropriate mutant enzymes was constructed. The positions chosen for mutation were residues 421 and 422. These residues lie approximately one turn further along the same α-helix from residue Gly^{418} and are completely inaccessible to solvent. They pack together in a cluster formed by residues Gly^{418}, Phe^{419}, Phe^{432}, Asp^{431}, Ala^{427}, Met^{425} and the same residues from the second subunit. The two-fold symmetry of the glutathione reductase dimer means that residue 421 is positioned opposite residue 422′ and 422 opposite 421′ (Figure 2). The nature of these interactions was exploited in the mutagenesis strategy. Mutation of both residues 421 and 422 to the same charged amino acid will juxtapose like charges (mutants $Val^{421} \rightarrow Glu:Ala^{422} \rightarrow Glu$, $Val^{421} \rightarrow Lys:Ala^{422} \rightarrow Lys$) whereas replacement of residue 421 with a positively charged amino acid and residue 422 with a negatively charged amino acid should juxtapose opposite charges (mutant $Val^{421} \rightarrow Lys:Ala^{422} \rightarrow Glu$). We also constructed a mutant ($Val^{421} \rightarrow His:Ala^{422} \rightarrow His$) that introduces bulky side chains with the potential to present opposing positive charges.

General properties of the mutant enzymes

Mutant enzymes were constructed and purified to homogeneity as described above. As judged by means of SDS/PAGE, all mutant enzymes were of the same apparent subunit molecular mass (Figure 3). However, when subjected to non-denaturing gel electrophoresis, all four mutant enzymes were found to migrate more slowly than the wild-type enzyme and as diffuse bands; there was no evidence for any protein band co-migrating with the wild-type enzyme (Figure 3). The buried nature of the amino acid residues undergoing replacement is reflected by the fact that there was no obvious effect of any change in charge on the electrophoretic mobility of the proteins during non-denaturing gel electrophoresis. However, the diffuse nature of the bands during electrophoresis suggests that these mutations at the dimer interface of glutathione reductase have adversely affected the overall structure of the enzyme dimer, indicating perhaps a partial unfolding of the polypeptide chain. However, all the mutant enzymes were found to be catalytically active when assayed for NADPH-dependent glutathione reduction at 30 °C. Given that a monomer of glutathione reductase cannot be active in this assay, the mutant enzymes can obviously form dimers.

The thermal stabilities of the mutant enzymes were investigated by performing enzyme assays after incubating the proteins for

Table 1 Thermal inactivation of wild-type and mutant glutathione reductases

The temperature at which 50% of the initial catalytic activity remained ($T_{50\%}$) after incubating the enzyme for 10 min at a series of increasing temperatures was measured from a plot of residual activity against temperature. The temperatures used were 4, 10, 20, 30, 40, 50, 60, 70 and 80 °C. The results are the mean of three independent measurements for each enzyme. For further details, see the text.

Enzyme	$T_{50\%}$
Wild-type	73±3
Gly^{418} → Trp	43*
Val^{421} → Glu:Ala^{422} → Glu	32±3
Val^{421} → Lys:Ala^{422} → Lys	40±4
Val^{421} → Glu:Ala^{422} → Lys	46±3
Val^{421} → His:Ala^{422} → His	49±2

* Data taken from [7].

10 min at various temperatures. As with the wild-type enzyme [4], all the mutant enzymes lost activity over a narrow temperature range, but the activity was lost at lower temperatures. The temperatures at which 50% of the initial activity remained ($T_{50\%}$) are presented in Table 1. It is clear that these mutations at the dimer interface are insufficient to prevent the formation of an active dimeric enzyme but that structural rearrangements to accommodate them must have occurred, as indicated by the loss of thermal stability.

Kinetic properties of the mutant enzymes

We demonstrated previously that the Gly^{418} → Trp mutation switches *E. coli* glutathione reductase from an enzyme displaying hyperbolic (Ping Pong) kinetics to one that exhibits highly sigmoidal behaviour (Hill coefficient 1.8) with respect to oxidized glutathione [7]. This sigmoidal behaviour was apparent only when the enzyme was assayed in the presence of a fixed non-saturating concentration of NADPH. The kinetic behaviour reverted to hyperbolic when NADPH was close to saturating concentrations. These results are in contrast with similar experiments on human glutathione reductase [21], where the mutation of residue Gly^{446} (equivalent to Gly^{418} in the *E. coli* enzyme) to a glutamate residue resulted in inactive and poorly folded monomers.

In the light of our previous observations on the *E. coli* mutant Gly^{418} → Trp, the detailed kinetic behaviour of the Val^{421}-Ala^{422} mutants was studied at a high (400 μM) and low (50–100 μM)

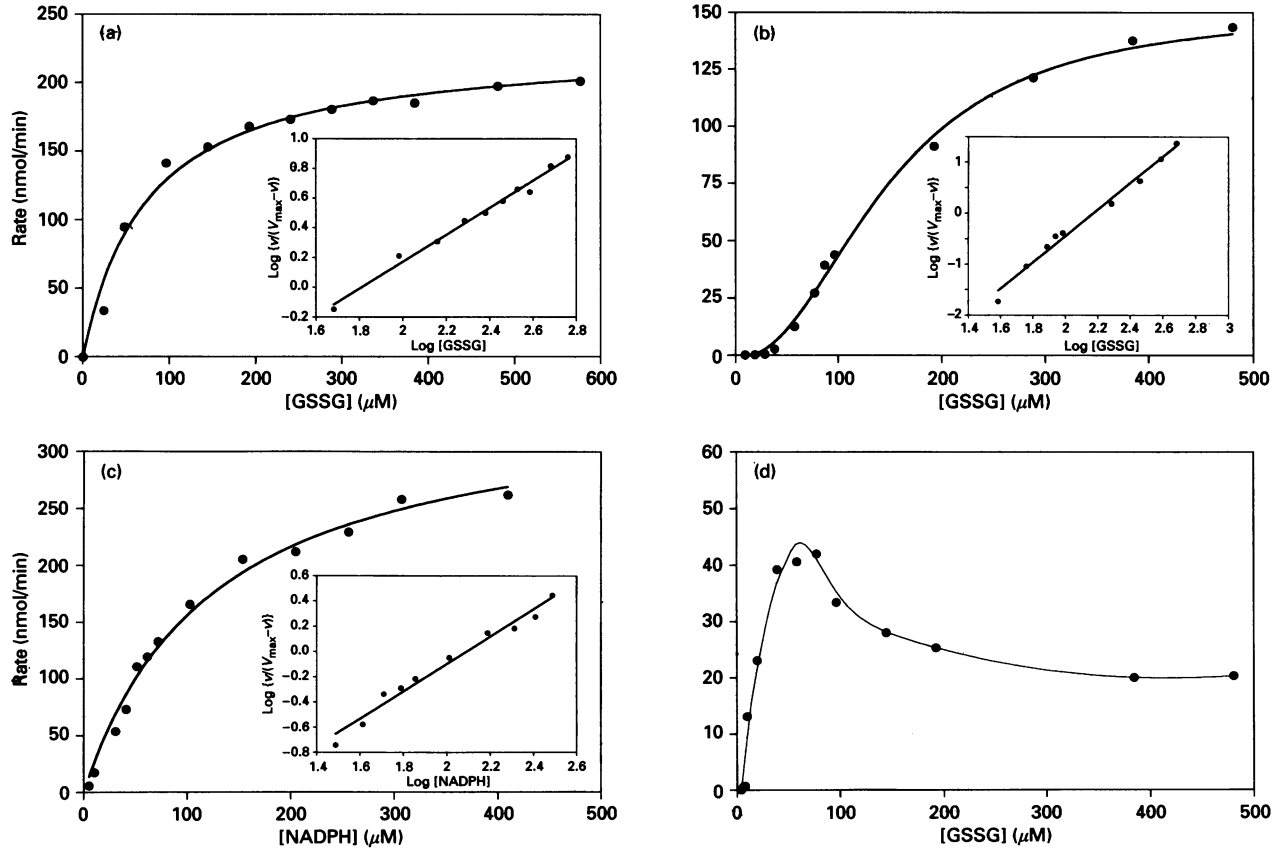

Figure 4 Plots of velocity against substrate concentration for the Val^{421} → His:Ala^{422} → His mutant enzyme

(**a**) NADPH concentration was fixed at 400 μM and glutathione concentration was varied. Data were fitted to a rectangular hyperbola. Inset, Hill plot of the same data. (**b**) NADPH concentration was fixed at 50 μM and glutathione concentration was varied. Data were fitted to a sigmoidal rate equation. Inset, Hill plot of the same data. (**c**) Glutathione concentration was fixed at 2 mM and NADPH concentration was varied. Data were fitted to a rectangular hyperbola. Inset, Hill plot of the same data. (**d**) Glutathione concentration was fixed at 20 μM and NADPH concentration was varied. Qualitatively similar plots were obtained for the other mutant enzymes described in this paper.

Table 2 Hill coefficients for wild-type and mutant forms of *E. coli* glutathione reductases at high and low fixed concentrations of NADPH

Kinetic profiles were generated by varying the glutathione concentration at each fixed concentration of NADPH, and Hill coefficients were calculated from the gradient of plots of $\log\{v/(V_{max}-v)\}$ against log[GSSG] in the linear region.

Enzyme	[NADPH](μM)	Hill coefficient
Wild-type	100	1.0
$Gly^{418} \rightarrow Trp$	100	1.8
	400	1.0
$Val^{421} \rightarrow Glu : Ala^{422} \rightarrow Glu$	100	2.1
	400	1.1
$Val^{421} \rightarrow Lys : Ala^{422} \rightarrow Lys$	50	2.1
	400	1.0
$Val^{421} \rightarrow Lys : Ala^{422} \rightarrow Glu$	50	2.1
	400	1.0
$Val^{421} \rightarrow His : Ala^{422} \rightarrow His$	50	2.5
	400	0.9

fixed concentrations of NADPH while varying the concentration of GSSG; and conversely, at high (20 mM) and low (20 μM) fixed concentrations of GSSG while varying the concentration of NADPH. At elevated concentrations of NADPH, the wild-type enzyme and all the mutant enzymes displayed hyperbolic kinetic behaviour (Hill coefficients of 1.0) when the concentration of glutathione was varied (Figure 4a and Table 2). The apparent kinetic parameters measured in the hyperbolic regime (Table 3) indicate that the apparent Michaelis constant for NADPH is substantially altered only for the $Val^{421} \rightarrow His : Ala^{422} \rightarrow His$ and $Val^{421} \rightarrow Lys : Ala^{422} \rightarrow Glu$ mutant enzymes. The apparent K_m for glutathione is raised by a factor of about 3- to 4-fold in the mutant enzymes and the apparent k_{cat} ranges from 5800/min to 15500/min for the mutant enzymes, compared with 16000/min for the wild-type enzyme. It is clear that *E. coli* glutathione reductase is not severely crippled as an enzyme by these mutations. In contrast, at the lower concentrations of NADPH, the kinetic behaviour of all the mutant enzymes was transformed to highly sigmoidal, with Hill coefficients of about 2 (Figure 4b and Table 2) obtained from plots of $\log[v/(V_{max}-v)]$ against log [GSSG]. The kinetic behaviour is thus controlled by the concentration of the fixed substrate NADPH.

When oxidized glutathione was fixed at a concentration of 2 mM and the concentration of NADPH was varied, hyperbolic kinetic behaviour was again observed (Figure 4c). However, when the glutathione concentration was fixed at the lower concentration of 20 μM and the concentration of NADPH was again varied, complex kinetic behaviour was observed. In this instance, the reaction velocity initially increased with NADPH concentration, reached a maximum and then subsequently declined at higher concentrations of NADPH (Figure 4d). Similar kinetic responses to changes in substrate concentrations were also seen for the $Gly^{418} \rightarrow Trp$ mutant enzyme (results not shown).

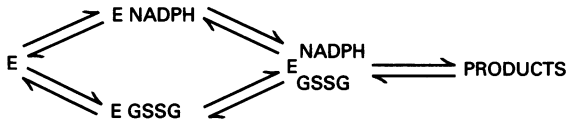

Scheme 1

Kinetic mechanism of the mutant enzymes

The overall kinetic response of the mutant enzymes as a function of substrate concentration is entirely consistent with a switch in kinetic mechanism from the Ping Pong mechanism displayed by the wild-type enzyme [5] to a random ternary complex mechanism (Scheme 1) in which the breakdown of the central complex is not the sole rate-determining step [22,23].

In this scheme, the favoured kinetic route is the one in which oxidized glutathione binds before NADPH. At low concentrations of NADPH the enzyme will be present in two forms, E–NADPH, and free enzyme, E. On the addition of glutathione, free enzyme either associates with GSSG and enters the more favourable kinetic pathway or GSSG binds to E–NADPH and follows the less favourable pathway. The effect is to have two competing pathways and, as the glutathione concentration is raised, more enzyme is diverted into the kinetically more favourable pathway. As the glutathione concentration is increased further, the enzyme becomes saturated with glutathione and the reaction velocity curve reaches a plateau. This generates a sigmoidal relationship between velocity and glutathione concentration (Figure 4b).

This kinetic model also predicts that at low concentrations of oxidized glutathione, the velocity of the reaction first increases as

Table 3 Steady-state kinetic parameters for wild-type and mutant forms of *E. coli* glutathione reductase

All assays were performed in the 'hyperbolic' regime and data were fitted to the Michaelis–Menten equation. The apparent K_m for NADPH was determined using a fixed and near-saturating concentration of glutathione (2 mM). The apparent K_m for glutathione and the apparent k_{cat} were determined at near-saturating concentrations of NADPH (values shown in parentheses). Data for the $Gly^{418} \rightarrow Trp$ mutant and the wild-type enzyme are taken from [7].

Enzyme	Apparent K_m for NADPH (μM)	Apparent K_m for GSSG (μM)	Apparent k_{cat} (per min)
Wild-type	22±2	97±12 (100 μM)	16000±350 (100 μM)
$Gly^{418} \rightarrow Trp$	41±5	311±33 (400 μM)	10200±900 (400 μM)
$Val^{421} \rightarrow Glu : Ala^{422} \rightarrow Glu$	10.3±0.5	505±58 (400 μM)	14900±1600 (400 μM)
$Val^{421} \rightarrow Lys : Ala^{422} \rightarrow Lys$	17.1±1.4	275±15 (400 μM)	19300±300 (400 μM)
$Val^{421} \rightarrow Lys : Ala^{422} \rightarrow Glu$	100±9	484±24 (400 μM)	5800±90 (400 μM)
$Val^{421} \rightarrow His : Ala^{422} \rightarrow His$	125±13	74±10 (400 μM)	15500±510 (400 μM)

NADPH increases, then peaks and finally decreases to a plateau region. These changes reflect flux initially passing through the more favourable pathway, but as the NADPH concentration increases an optimum is reached as substrate is diverted through the less favourable pathway. Eventually, all flux will pass through the less favourable pathway because the enzyme becomes saturated with NADPH. In this regime, the velocity curve reaches a plateau (Figure 4d). At near-saturating concentrations of NADPH or GSSG, the kinetic behaviour is best described as hyperbolic. In this case, little free enzyme exists and only one of the kinetic pathways is followed (Figures 4a and 4c).

Conclusions

The effects of these mutations, in which various charges, both like ($Val^{421} \rightarrow Lys$:$Ala^{422} \rightarrow Lys$ and $Val^{421} \rightarrow Glu$:$Ala^{422} \rightarrow Glu$) and unlike ($Val^{421} \rightarrow Lys$:$Ala^{422} \rightarrow Glu$), have been introduced into the upper interface region of *E. coli* glutathione reductase, are directly comparable with those reported previously for the $Gly^{418} \rightarrow Trp$ mutant [7]. We would expect that significant structural rearrangements would be generated by electrostatic repulsion between the side chains of amino acid residues with like charges in such a tightly packed region of the subunit interface. These rearrangements, although remote from the active site, are evidently sufficient to cause alterations in the steady-state kinetic parameters and to have profound effects on the steady-state kinetic mechanism of the enzyme.

The kinetic behaviour of the $Val^{421} \rightarrow His$:$Ala^{422} \rightarrow His$ mutant was also strongly sigmoidal with respect to glutathione at low concentrations of NADPH. Given that the two histidine residues have been introduced into a buried hydrophobic region of the dimer interface, we are unable to determine whether the imidazole side chains are protonated under the conditions of the steady-state kinetic assays. Thus, in this mutant, it may be that the structural perturbation is a consequence of opposing positive charges or steric interactions, or a combination of both. We attempted to address this question by creating the $Val^{421} \rightarrow Lys$:$Ala^{422} \rightarrow Glu$ mutant, in which the opposite charges are neutralizing but steric perturbation is retained. The $Val^{421} \rightarrow Lys$:$Ala^{422} \rightarrow Glu$ mutant, like the other mutants described above, displayed strongly sigmoidal kinetic behaviour with respect to glutathione, suggesting that the steric interactions required to accommodate two bulky side chains are probably more important than any additional effect induced by electrostatic repulsion between them.

This work demonstrates that *E. coli* glutathione reductase can undergo several changes of kinetic mechanism, departing from the wild-type Ping Pong and appearing as ordered sequential [8] or random ternary complex ([7] and this paper), in response to the replacement of one or more particular amino acids. Such plasticity of kinetic mechanism was hitherto unforeseen and must be associated with a comparable plasticity of protein structure. The precise structural changes underlying these effects remain to be determined. A manifestation of the assumed structural rearrangement is found in the decreased thermal stabilities of all the dimer interface mutants compared with the wild-type enzyme. A fuller understanding of these differences and the structural rearrangements accompanying the changes in kinetic behaviour must await crystallographic analysis of one or more of the mutant proteins.

We thank the former Science and Engineering Research Council and The Royal Society for financial support, and the Cambridge Centre for Molecular Recognition, funded by the Biotechnology and Biological Sciences Research Council and The Wellcome Trust, for the provision of facilities. The valuable collaboration of Mr M. J. Cockerill in some of the early experiments is gratefully acknowledged. A. Bashir was supported by an SERC Research Studentship and Wolfson College, Cambridge. N.S.S. is a Royal Society 1983 University Research Fellow. A. Berry was a Royal Society 1983 University Research Fellow.

REFERENCES

1 Greer, S. and Perham, R. N. (1986) Biochemistry **25**, 2736–2742
2 Akerboom, T. P. M., Bilzer, M. and Sies, H. (1982) J. Biol. Chem. **257**, 4248–4256
3 Meister, A. (1989) in Coenzymes and Cofactors, vol. 3A (Glutathione), pp. 1–48, Wiley, New York
4 Scrutton, N. S., Berry, A. and Perham, R. N. (1988) FEBS Lett. **241**, 46–50
5 Deonarain, M. P., Berry, A., Scrutton, N. S. and Perham, R. N. (1989) Biochemistry **28**, 9602–9607
6 Scrutton, N. S., Berry, A., Deonarain, M. P. and Perham, R. N. (1990) Proc. Roy. Soc. Lond. B **242**, 217–224
7 Scrutton, N. S., Deonarain, M. P., Berry, A. and Perham, R. N. (1992) Science **258**, 1140–1143
8 Berry, A., Scrutton, N. S. and Perham, R. N. (1989) Biochemistry **28**, 1264–1269
9 Scrutton, N. S., Berry, A. and Perham, R. N. (1990) Nature (London) **343**, 38–43
10 Henderson, G. B., Murgolo, N. J., Kuriyan, J. et al. (1991) Proc. Natl. Acad. Sci. U.S.A. **88**, 8769–8773
11 Leistler, B. and Perham, R. N. (1994) Biochemistry **33**, 2773–2781
12 Mittl, P. R. E. and Schulz, G. E. (1994) Protein Sci. **3**, 799–809
13 Mittl, P. R. E., Berry, A., Scrutton, N. S., Perham, R. N. and Schulz, G. E. (1993) J. Mol. Biol. **231**, 191–195
14 Mittl, P. R. E., Berry, A., Scrutton, N. S., Perham, R. N. and Schulz, G. E. (1994) Protein Sci. **3**, 1504–1514
15 Sambrook, J., Fritsch, E. F. and Maniatis, T. (1989) Molecular Cloning: A Laboratory Manual, Cold Spring Harbor Laboratory Press, Cold Spring Harbor, NY
16 Deonarain, M. P., Scrutton, N. S. and Perham, R. N. (1992) Biochemistry **31**, 1491–1497
17 Scrutton, N. S., Berry, A. and Perham, R. N. (1987) Biochem J. **245**, 875–880
18 Laemmli, U. K. (1970) Nature (London) **227**, 680–685
19 Ornstein, L. (1964) Ann. N.Y. Acad. Sci. **121**, 321–349
20 Davis, B. J. (1964) Ann. N.Y. Acad. Sci. **121**, 404–427
21 Nordhoff, A., Bücheler, U. S., Werner, D. and Schirmer, R. H. (1993) Biochemistry **32**, 4060–4066
22 Segel, I. H. (1975) in Enzyme Kinetics, pp. 460–461 and 646–659, Wiley Interscience, New York
23 Ferdinand, W. (1966) Biochem. J. **98**, 278–283
24 Kraulis, P. J. (1991) J. Appl. Crystallogr. **24**, 946–958

Received 4 May 1995/28 July 1995; accepted 2 August 1995